Analytical Biochemistry 561–562 (2018) 1–10

Contents lists available at ScienceDirect

Analytical Biochemistry

journal homepage: www.elsevier.com/locate/yabio

An electrochemical biosensor to distinguish between normal and cancer cells based on monitoring their acidosis using gold-coated silicon Nano-roughened electrode

Alireza Alikhani[a,b,1], Milad Gharooni[a,b,1], Hassan Moghtaderi[a,e,2], Fatemeh Farokhmanesh[c,d,2], Hamed Abiri[a,b], Mona Salimi[e], Farnoosh Attari[f], Mohammad Abdolahad[a,b,*]

[a] Nano Electronic Center of Excellence, Thin Film and Nanoelectronic Lab, School of Electrical and Computer Eng, University of Tehran, Tehran, Iran, P.O. Box 14395/515, Tehran, Iran
[b] Nano Electronic Center of Excellence, Nanobioelectronic Devices Lab, School of Electrical and Computer Eng., University of Tehran, Tehran, Iran, P.O. Box 14395/515, Tehran, Iran
[c] Department of Electrical Engineering, Yazd University, Yazd, 89195-741, Iran
[d] Department of Biotechnology, Pasteur Institute of Iran, Tehran, Iran, P.O. Box 1316943551, Tehran, Iran
[e] Physiology and Pharmacology Department, Pasteur Institute of Iran, Tehran, Iran, P.O. Box 1316943551, Tehran, Iran
[f] Department of Animal Biology, School of Biology, College of Science, University of Tehran, Tehran, Iran, P.O. Box 19395-4644, Tehran, Iran

ARTICLE INFO

Keywords:
Electrochemical sensor
pH
Membrane depolarization
Silicon nano-roughened
Cancer cell
Acidosis

ABSTRACT

One of the most interesting fields of research in cancer diagnosis is tracing the relation between extracellular media and cancer progression. Detecting the secreting contents of the cells and translating these molecular identifications into label-free recognizable patterns would open new opportunities in cancer research. Electrochemical responses are in the range of most attractive sensing mechanisms especially in biochemical approaches. Perturbed ionic exchanges as a known biochemical function of cancer cells presented a strong correlation with the pH of the tumor microenvironment. Different ionic activities detected by an electrochemical bio-sensing system in the malignant and normal cells in the presence of acidic ambient were our main results presented in this research. Herein, silicon Nano-roughened substrate as a well-known electrochemical interface was applied in the construction of the biosensor. Viability rate as well as apoptotic factors involving in cancer progression were assessed by biochemical assays in normal (MCF10A) and cancer (MCF7 and MDA-MB468) breast cells. Our findings demonstrated that pH-based electrochemical responses were matched with the results obtained from the biological analyses of both normal and malignant cells. Induction of acidosis in the cells followed by monitoring their electrochemical responses would be a new trend in microenvironment based cancer investigation.

1. Introduction

A bio-electrochemical sensor can translate the cell chemical phenomena into an electrical signal [1]. Label-free tracking of such chemical signatures is of great importance since the presence of the biological markers (like enzyme, antibodies and etc.) in the traditional techniques might seriously affect the resultant response [2,3]. Moreover, the complexity of chemical modifications would limit the accuracy and reliability of the bio-electrochemical sensor while achieving selective label-free interactions between analytics (the complex of the cell and its medium) and the examined interface (the cell culture surface), can lead to great responses with minimized perturbations and maximized precision. Among various models of electrochemical bio-sensing, detection of alterations in the oxidative/reductive responses of the analytic as a result of changes in the extracellular media, attracted great interest in the recent years [4,5]. Engineering the bio-electrochemical interface in a label-free bio-sensing manner could be crucial to obtain the accurate and stable responses [6,7]. It has been reported that

* Corresponding author. Nano Electronic Center of Excellence, Thin Film and Nanoelectronic Lab, School of Electrical and Computer Eng, University of Tehran, Tehran, Iran, P.O. Box 14395/515, Tehran, Iran.
E-mail address: m.abdolahad@ut.ac.ir (M. Abdolahad).
[1] Authors with same collaboration.
[2] Authors with same collaboration.

https://doi.org/10.1016/j.ab.2018.09.005
Received 10 June 2018; Received in revised form 3 September 2018; Accepted 5 September 2018
Available online 13 September 2018
0003-2697/

applying Nano-textured surfaces would enhance both sensitivity and selectivity of the biosensors [8].

Extracellular media as one of the most interesting analytics could reflect many biological parameters of active bio-agents such as cells and has an important role in modifying their behavior [9]. For example, acidification (reduction in the pH of the extracellular media) could induce many functional changes correlated with the phenotype of the cells [10,11], as many evidences validated that the most acidic tumors are more prone to invasion and metastasis formation [12]. Activation of autophagy in the acidified cancer cells increases the probability of their invasion [13], whereas an aberrant increase of intercellular H^+ in normal cells perturbs their ionic equilibrium and would induce apoptotic pathways [14].

Tracing the effects of acidic extracellular media on normal and cancer cells by high-resolution electrochemical approach has not be discussed in previous reports. Therefore, in the current study, we introduce for the first time a bio-electrochemical sensing method to monitor the pH-dependent behavior of normal and cancer cells by tracing their biochemical properties, ionic exchanges, and oxidation/reduction interactions in order to diagnose the invasive tumor cells. The intensity of oxidation/reduction exchanges and electrical current blocking are our main monitoring parameters. The work electrodes of our sensor were fabricated by silicon Nano-roughened (SiNR) substrate which could produce an enhanced interactive interface to improve signal extraction from the adhered cells [15]. The crystalline structure, high interactive surface and stable physical and chemical properties of the work electrode in a moderate acidic media, were some of the advantages of the selected SiNRs as our candidate for the cellular interface [16,17]. The cells were cultured on the SiNRs electrodes and subsequently, the pH of the medium was reduced to the acidic values (6.5 & 5.5) for the known time intervals. The cyclic voltammetry (CV) and differential pulse voltammetry (DPV) of the cultured cells were extracted up to 24hr. In parallel, biological analyses were experimented to evaluate the correlation between electrical signals and biological evidences.

2. Material and methods

2.1. Fabrication of the biosensor

The Si samples as a substrate were cleaned through RCA1 standard cleaning process (NH4OH:H2O2:H2O solution with a volume ratio of 1:1:5, respectively). Subsequently, a thin layer ($\sim$300 nm) of SiO_2 was grown on the substrate by the wet oxidation furnace. To define the Nano-roughened work electrode, a 1 μm photoresist layer was deposited on the surface of the sample and circle area was patterned by the developer. The anisotropic dry etching method used in this study is based on sequential deep reactive ion etching (DRIE) process which utilizes SF_6 gas for etching step and a mixture of hydrogen and oxygen with a trace value of SF_6 instead of polymeric material in the passivation (Table 1). This process enjoys low plasma power density and higher reactor pressure in comparison to Bosch process. Fig. 1-B schematically, demonstrates Nano-roughening mechanism used in the sequential etching process and main ions and radicals which have effects are shown. Fluorine ions and radicals are the primary etching agents to react with silicon atoms from the top surface layer gradually to inside layers, while oxygen and hydrogen ions and radicals combined together comprise the building blocks to synthesize the complex quasi silicon oxide compound on top of the surface layer. On the other hand, due to the directional nature of plasma, $SF5^+$ ions bombard the bottom of the sample and helped the removal of bottom passivation layer while sidewalls passivation was less affected (Fig. 1 B1).

Table 1
Plasma parameter in Nano-roughening process.

Process	Flow ($SF_6/O_2/H_2$) (sccm)	Power (W)	Time(s)
Etching	140/0/0	130	8
Passivation	13/230/620	200	50

Table 1 provides near-optimum conditions for both the passivation and etching sub-cycles in the deep etching process. In general, to achieve a high aspect ratio Nano-tips, one has to maintain a balance between the passivation parameters especially hydrogen and oxygen gases. Incorporation of H_2/O_2 and SF_6 during the passivation step leads to the formation of a protecting layer over the sample while hydrogen bombardment helps to remove this protective layer from the bottom of the crater. We have examined the effect of various parameters such as gas flow, plasma power, duration and pressure of each sub-cycle. It has been found that the reduction in the flows of both hydrogen and oxygen gases during the passivation step would lead to improper passivation which in turn leads to the improper formation of a grassy surface. By increasing the passivation time and power, sharp tips are obtained but the total etch rate drops (Fig. 1 B2).

Nano-roughening process induced Nano features with the diameter of sub 100 nm and height of about 100–150 nm (AFM (Atomic-force microscopy) profile) (Fig. 2). A thin layer of titanium and Au layer (20 and 200 nm, respectively) deposited by RF-sputtering system (Veeco Co.) and patterned by lithography process; therefore, the working electrode fabricated by Nano-roughened and reference and counter electrodes were coated by Au. The schematic of the fabrication process, as well as an AFM and SEM image of the sensor, are shown in Figs. 1 and 2.

2.2. Cell culture

MCF10A, MCF7 and MDA-MB468 cell lines, obtained from the National Cell Bank of Iran (Pasteur Institute), had been isolated from human breast normal, non-metastatic and metastatic tumors, respectively. MCF7 and MDA-MB468 cells were cultured in RPMI-1640 medium (Sigma) supplemented with 5% fetal bovine serum (Sigma), and 1% penicillin/streptomycin (Gibco). The MCF10A cell line was cultured in DMEM/F12 supplemented with 10% horse serum, 1% antibiotic solution, 0.2% NaHCO3, insulin (5 μg/ml), EGF (10 ng/ml) and Hydrocortisone (1 μg/ml). All cells were maintained in a humidified incubator at 37°C containing 5% CO_2 and the medium was renewed every other day. Prior to each experiment, medium of cells was removed, then 1% trypsin was added and after 5 min RPMI1640 were added, then the trypsinized cells were centrifuged (5 min, 1200 RPM). After removing medium, cells were counted and suspended on the washed sensor. To minimize the effect of trypsinization, the procedure was taken less than 4 min at room temperature around 20–22 °C. We held the samples in the incubator for 4hr to achieve cell attachment on the sensor work electrode.

2.3. CV measurement procedure

For CV characterization, three-electrode electrochemical cyclic voltammetry was performed using the electrochemical workstation, RNFPG Stat (Roshd Nanofannavaran Co. Iran). Instead of the system electrodes, we used our integrated electrodes fabricated as mentioned (Fig. 1 A). CV was performed between the integrated SiNR covered working and counter electrodes, with an on chip reference electrode. The reference electrode was calibrated before by Ag/AgCl reference electrode in 1 mM ferrocene carboxylic acid with 1 mM potassium chloride solution. CV studies were performed using DC voltage and no AC frequency was applied. For CV data recording, measurements were carried out at -0.4–0.8 V at a scan rate of (100 mv/s).

2.4. MTT assay

To investigate the biocompatibility of Nano-roughened surfaces, we

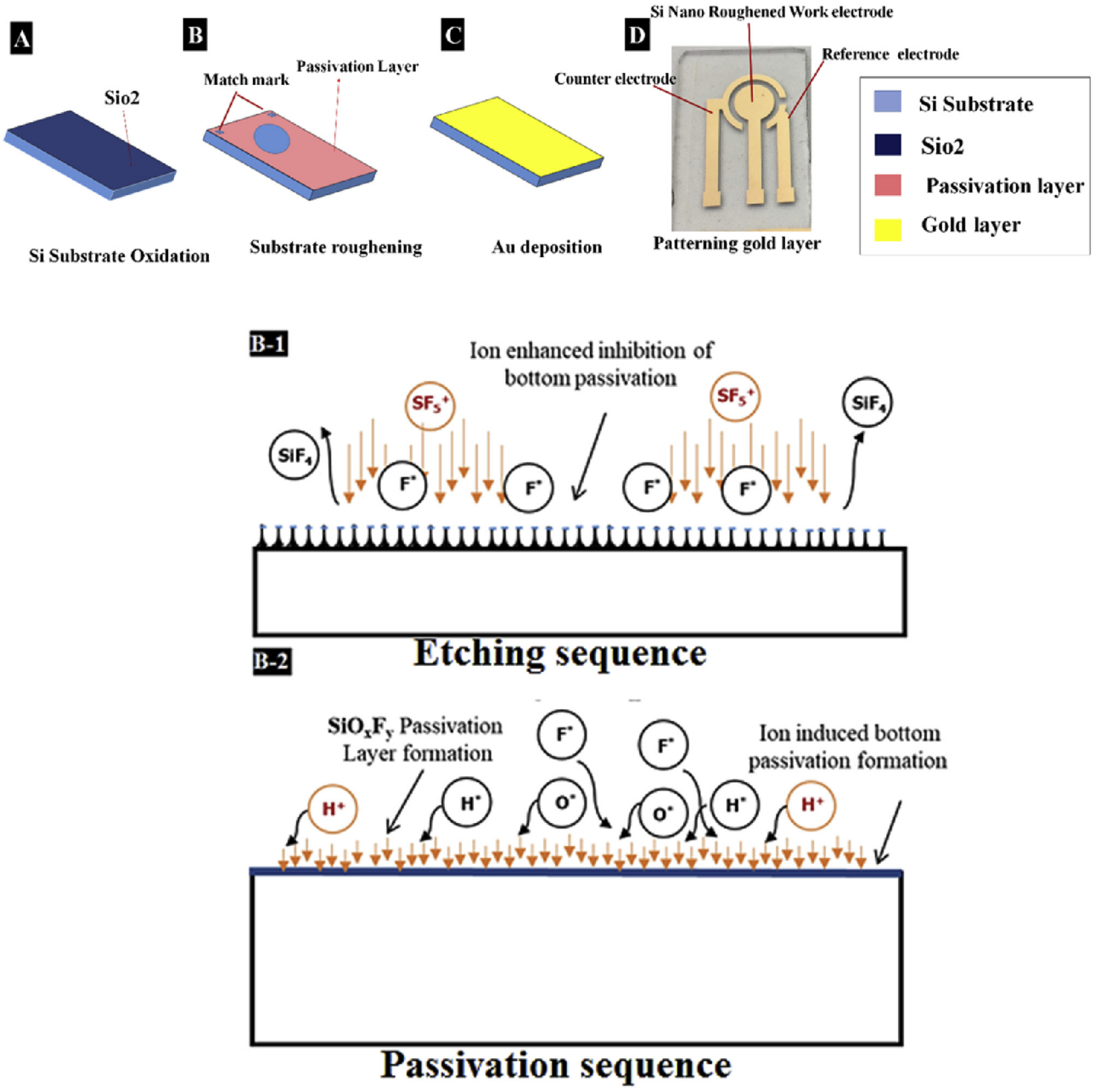

Fig. 1. Fabrication process of the sensors. (A-1) SiO2 has been grown on the Si surface for electrical isolation. (A-2) Photoresist layer has been coated as a mask of roughening process in DRIE plasma system. (A-3, 4) Nano-roughened working electrodes has been fabricated and Ti-Au have been deposited and patterned as references and counter electrodes. (B) Schematic of etching mechanism used in the Nano-roughening process. Main ions and radicals which have effect are shown. Nano-roughening process including (B-1) Etching sequence and (B-2) passivation sequence.

used a MTT (3-(4, 5-dim ethyl thiazol-2-yl)-2, 5-diphenyl tetrazolium bromide) assay. The surface of the device has been sterilized by autoclave before cell seeding process. The cells were attached on SiNR surface and after 24hr they were removed from the substrate by trypsin and the culture media was added to the cell solution. Subsequently, the cells were placed in the sterile 96-well microplates with the same concentration and the MTT protocol was applied on each well. This assay verifies the viability of the cells based on colorimetric measurement. The reduction of yellow tetrazole to purple formazan is related to the ratio of remained live cells. In this regard, 10 µl of MTT solution with the concentration of 5 mg/µl was added to each well and they were incubated for 4hr in 5% CO_2 ambient in 37 °C. Next, the float materials were removed from the surface of the wells and 100 µl of dimethylsulfoxiede was added to each well. After 20 min shaking of the plate (in order to solve the formazan), the optical absorption of each cell contained well was calculated at 493 nm by microplate reader system. The percentage of viable cells versus the control well and slope variation versus absorption diagram was indicated [18].

2.5. Annexin-V/PI

Apoptosis percentage was detected by Annexin V-FITC Apoptosis Detection Kit (ab14085, Abcam, Cambridge, UK). After culturing MCF10A, MCF7 and MDA-MB468 cell lines with different pH media (pH 6.5, 5.5), cells were trypsinized and collected by centrifugation and resuspended in 500 µl of binding buffer. In the next step, 5 µL of Annexin V-FITC and 5 µL of Propidium Iodide (PI 50 µg/ml) were added to the cells and after incubation in room temperature for 5 min dark, the

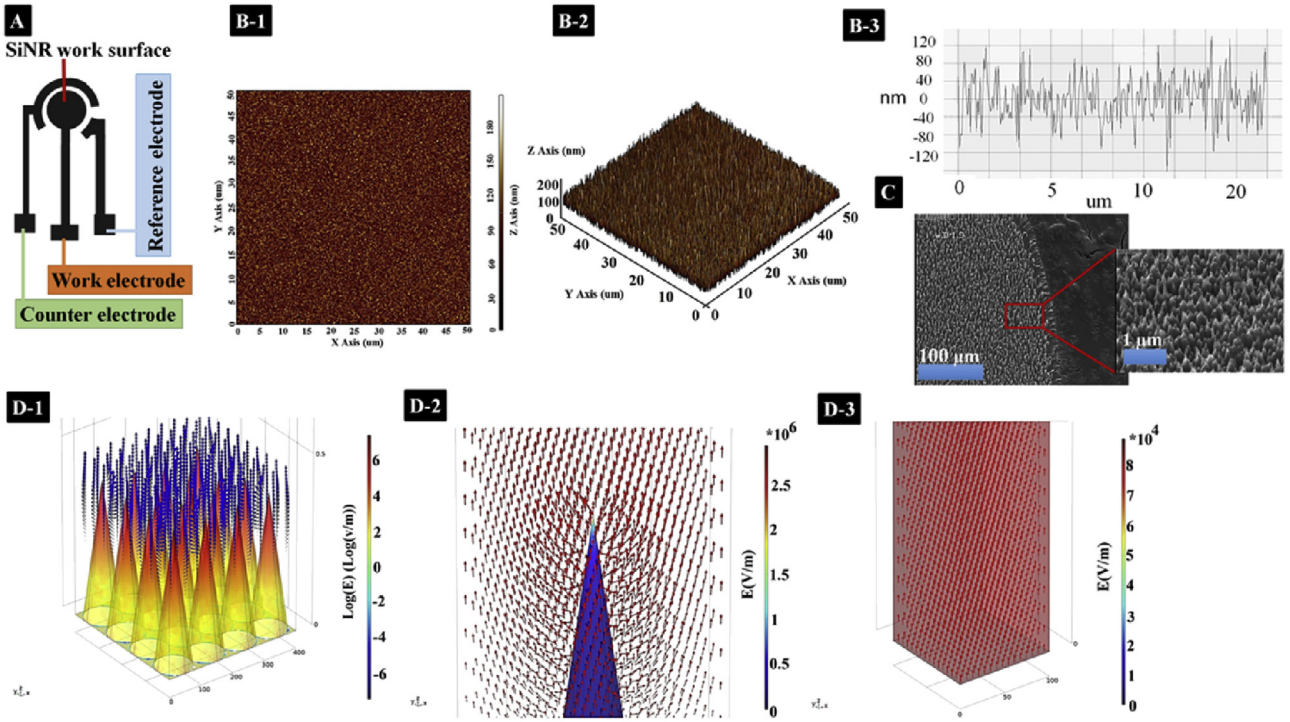

Fig. 2. Characterization of the electrochemical biosensor. (A) Schematic of the electrochemical sensor. (B-1 to B-3) AFM image of the Nano-roughened surface. (C) SEM image of the Nano-roughened work. (D) Simulation of the electrical field enhancement by Nano tips and finite element method. (D-1, 2) Logarithm of the electrical field for Nano-roughened surface and electrical field in the vector distribution in Nano pillars surface. (D-3) Electrical field distribution in planar surface.

fluorescent intensity was measured by the flowcytometery (FACScan Becton Dickinson, Mountain View, CA).

2.6. Apoptosis and flowcytometery analysis of cell cycle

For cell cycle investigation by flowcytometery, cells were washed in PBS and fixed in 70% methanol. Cells were then incubated with 20 µg/ml PI (Roche Diagnostics), and 10 µg/ml RNase (Sigma-Aldrich) at 37 °C for 30 min and cell cycle analysis was performed using an EPICS Profile II flow cytometer (Coulter Corp., Miami, FL) with the Multicycle Phoenix Flow Systems program (San Diego, California).

2.7. Detection of intracellular reactive oxygen species (ROS) levels

Intracellular ROS were spotted using an oxidation-sensitive fluorescent probe dye, 2, 7-dichlorodihydro fluorescein diacetate (DCFD). Concisely, 1×10^6 cells were incubated in a 60 mm culture dish. The cells were then washed in PBS and incubated for 30 min at 37 °C with PBS containing 20 µM DCFD. The samples were analyzed using a FACScan flowcytometer [19].

2.8. Nitrite (NO_2^-) detection

For evaluation of the amount of NO release, we utilized Griess reagent under acidic conditions to record the accumulated nitrite (NO_2^-), which is a stable breakdown product of NO. During the assay, medium aliquots were mixed with equal volumes of Griess reagent and incubated at room temperature for 15 min. To analyze the azo dye production, a spectrophotometer with absorbance set at 490 nm was used. Sodium nitrite was used as a standard [20].

2.9. Measurement of the mitochondrial membrane potential (MMP)

MMP was assessed by applying rhodamine 123 as a fluorescent dye (Ex/Em = 485/535 nm). After treatment, the cells were trypsinized and suspended in 1 ml PBS. Next, 3 ml of 1 mg/ml rhodamine 123 was added to cell suspension and incubated for 10 min at 25 °C. The cells were then washed twice with PBS and were observed with a fluorescence microscope (Zeiss, Germany) at 200 magnifications. Also, MMP was measured using a FACStar flow cytometer as previously described. In brief, 1×10^6 cells in a 60 mm culture dish were incubated and then were washed twice with PBS and incubated with rhodamine 123 (0.1 mg/ml) at 37 °C for 30 min. The absence of rhodamine 123 from cells showed the loss of MMP in the cells.

2.10. SEM methodology

To prepare samples for SEM, after electrical measurement and washing thoroughly by PBS, the cells were fixed with glutaraldehyde (5%) solution for 5 min followed by drying in the air ambient. The fixed samples were coated by Au (in DC Sputtering system) with the height of 10 nm to increase resolution.

3. Results and discussion

3.1. Characterization of Si nano-roughened surface

The applied SiNR substrate in our biosensor, leading to increase of the active electrical interface between the cultured cells and the sensor (Fig. 2 A), was morphologically characterized by atomic force microscopy (Fig. 2 B) and field emission scanning electron microscopy (Fig. 2 C). Our results revealed that Nano-roughening increased the roughness of the surface to about 120 nm providing an enhanced interface with the cellular media to better track any ion exchange regarding the biological processes. This high resolution ion exchange tracing could subsequently provide us with an enhanced sensitivity to detect a minor produced electrical current, which in turn results in an electrochemical response of the sensor (Fig. 2).

As shown in Fig. 2D, simulation based on analytical software demonstrates the electric field enhancement in the biased SiNR substrate

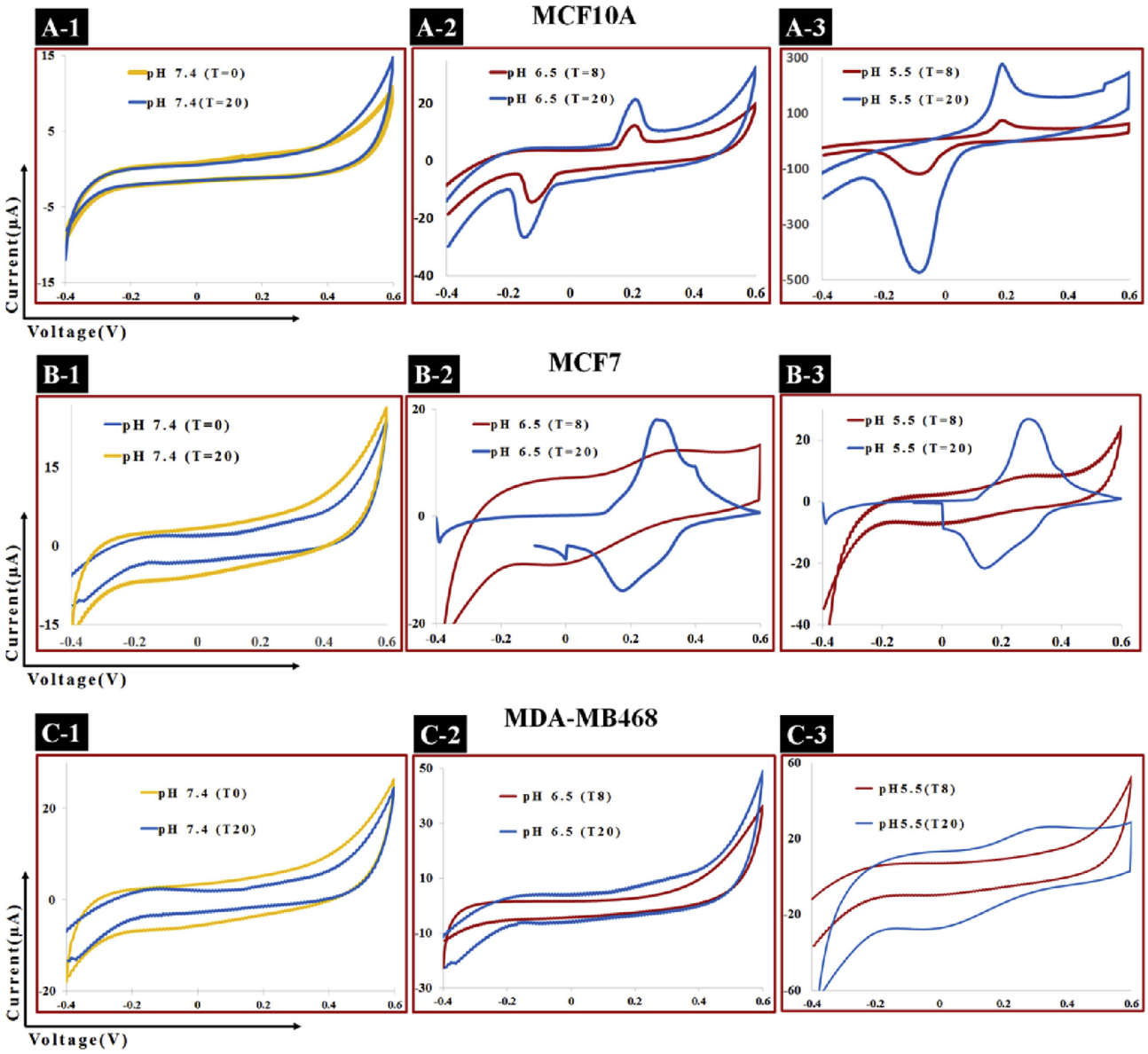

Fig. 3. Cyclic voltammetry (CV) responses of MCF10A, MCF7 and MDA-MB468 cells cultured on Nano-roughened sensors after 4hr of incubating in acidic media (pH 6.5 and 5.5) compared to normal ambient (pH 7.4). The culture medium of the cells was renewed after 4hr and the current measurements were carried out in time intervals of 4hr–24hr. (A-1) CV signals in MCF10 cells in normal pH. (A-2) Semi reversible anodic/cathodic peaks in MCF10 cells in pH 6.5. (A-3) Sharper peaks in MCF10 cells in pH 5.5 which means that an ionic electrochemical reaction proceeded in the acidic media and got progressed in the lower pH. (B-1) CV signal for the MCF7 cells in the normal pH. (B-2 and B-3) Recorded current measurements for MCF7 cell line in pH 6.5 and 5.5 shows a detectable trace of peaks at T20. (C-1) CV signal for the MDA-MB468 cells in the normal pH. (C-2, C-3) Recorded measurements for MDA-MB468 cell line in pH 6.5 and 5.5.

with respect to the planar smooth Si surface. The results obtained from finite element simulation showed that the electrical field for Nano-roughened surface is about four times greater than that of the planar surface (Fig. 2 D1 vs. D3).

Our results suggest for the first time a quick and simple fabrication method for a high resolution biosensor using electrochemical approach.

3.2. Response of the sensor in the presence of cancer cells

The SiNRs were settled in the culture dishes and then the trypsinized cells were seeded on the SiNR work electrodes and incubated in normal media (pH 7.4) for 4hr for them to completely adhere to the electrode. Following addition of two acidic media with pH 5.5 and 6.5 to the adhered cells on the sensor, cyclic voltammetry (CV) and differential pulse voltammetry (DPV) signals were extracted at time intervals of 12 and 24hr. The ionic culture media RPMI1640 (enriched 10% FBS) was employed for the culture of cancer cells. Therefore, the base electrochemical response of this media must be considered in all of the analyses. Previously, we have shown that the electrochemical response of RPMI media appeared at 200 mV [15,17]. The extracted CV signal from the acidified normal cells (MCF10A) exhibited an increase in the oxidation/reduction peak and in the electrical current compared to that of untreated control cells (Fig. 3 A). It is worth to mention that breast cancer cells, MCF7 behave similar to the normal breast cells (MCF10A) (Fig. 3 B), but with a lower slope. However, the CV profile of MDA-MB468 metastatic cells at pH 6.5 displayed a similar behavior to that of the control, whereas the presence of an oxidation/reduction peak at pH 5.5 could not be neglected (Fig. 3 C). The reason that there is no anodic/cathodic peak in all of the untreated control cells (Fig. 3 A1, B1, C1) is that the compact monolayer of the attached cells on the work electrode does not allow the current flow to happen and as a result, the current blocking occurs. Thus the increment of the electrochemical

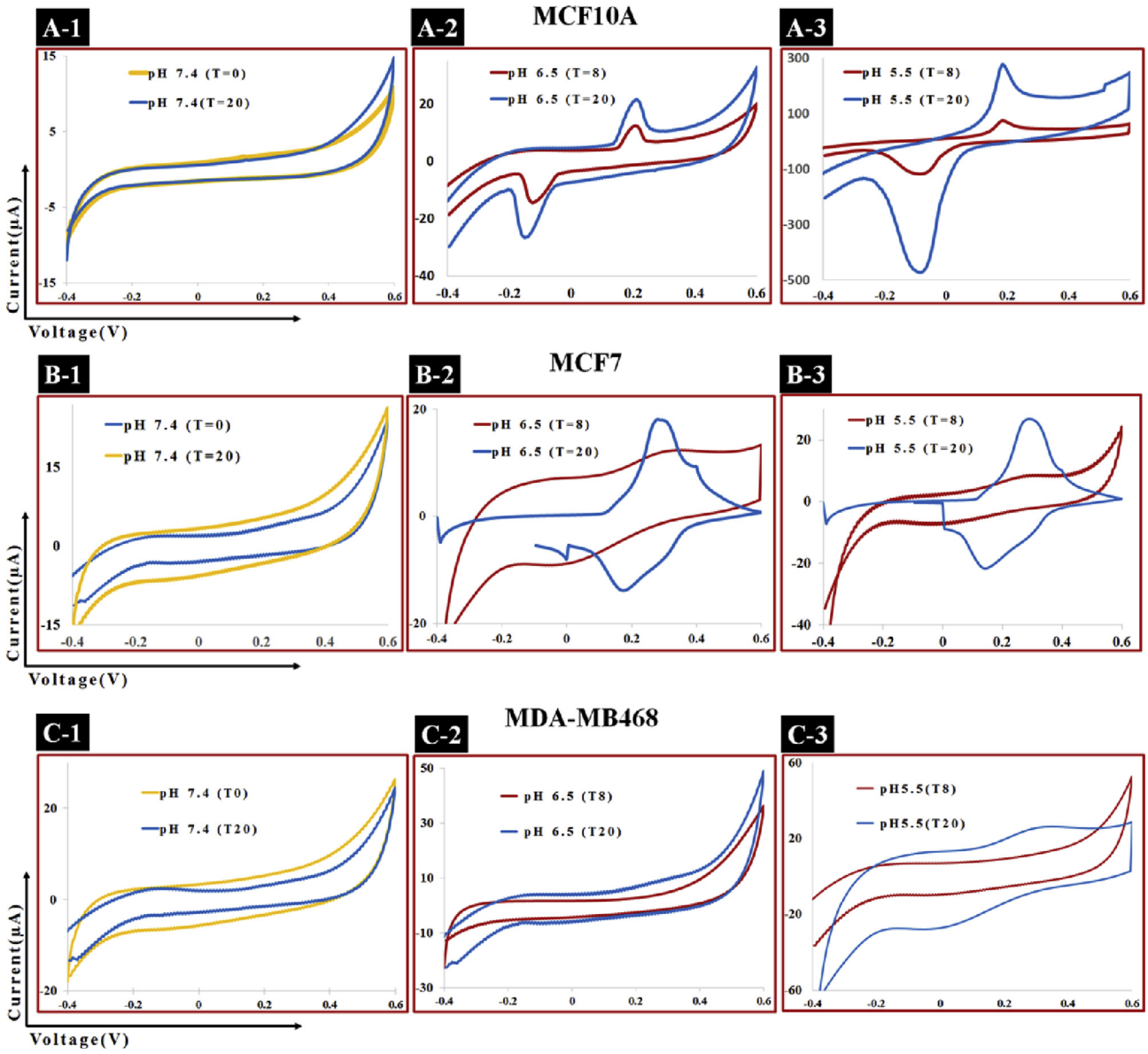

Fig. 3. (*continued*)

response peak observed in the MCF10A and MCF7 in the acidified media implies that the cells undergone apoptosis and were detached from the work electrode; as a result, the electrode can detect the whole or a part of the RPMI culture media and the CV profile gets similar to that of RPMI solution (Fig. 3 A2-3, B2-3). The intensity of the oxidation/reduction peaks can be correlated to the percentage of apoptosis and maintenance of cell viability as confirmed by all the biological assays (Figs. 7 and 8). Therefore, the lack of electrochemical peaks in the metastatic MDA-MB468 cells in pH 6.5 and pH 5.5 (T0-T8) is equal to their resistance to apoptosis (Fig. 3 C2, 7 B2, 7 D2, 8 B2), yet longer treatments in pH 5.5 would lead to peak emergence and apoptosis initiation (Fig. 3 C3).

In line with our results, it is reported formerly that in the acidified media, normal cells try to maintain their viability, but augmentation of the H^+ ion triggers acidosis and would result in the apoptosis induction [21]. Nonetheless, cancer cells depending on their metastatic grades tend to electrically maintain their intercellular space more positive in order to conserve their membrane depolarization and to precede the mitosis process. Membrane depolarization is a phenomenon in which proliferating cells regarding their invasiveness tend to maintain their intercellular ambient more positive with exchanging of Na^+ and Cl^- ions [22–24].

Given the above report and considering our data we suggest that induction of extracellular acidic media along with employing Nano structured and bio-compatible electrode could trace the activated ion exchange (Fig. 4 A). On the other hand, facilitated diffusion due to membrane depolarization would result in increasing the activity of BT (HCO_3^-) and NBC (Na^+/HCO_3^-) transporters followed by the entrance of Na^+ and exit of Cl^- into and out of the cell, respectively [25]. Importantly, it has been reported that non desired entrance of HCO_3^- into the cancer cells (Fig. 4 B1) is a phenotype related evidence in which $HCO3^-$ reacts with the produced H^+ leading to the production of H2O and CO2, which interestingly can neutralize the aberrant effect of the intercellular H^+ ion [25]. Consequently, no H^+ might remain in the MDA-MB468 cells at pH 6.5, which results in the similarity of the CV signals obtained from this cell line at pH 6.5 and 7.4, suggesting that these cells could recapitulate their viability at pH 6.5 (Fig. 3 C2). It is worth mentioning that as the result of H^+ over production at pH 5.5, a trace of electrochemical peak could be recorded from the acidified MDA-MB468 cells (Fig. 3 C3). As expected, the intensity of such peaks in these cells was lower compared to those of observed in acidified MCF7 cells due to the lower internal $HCO3^-$ concentration as the H^+

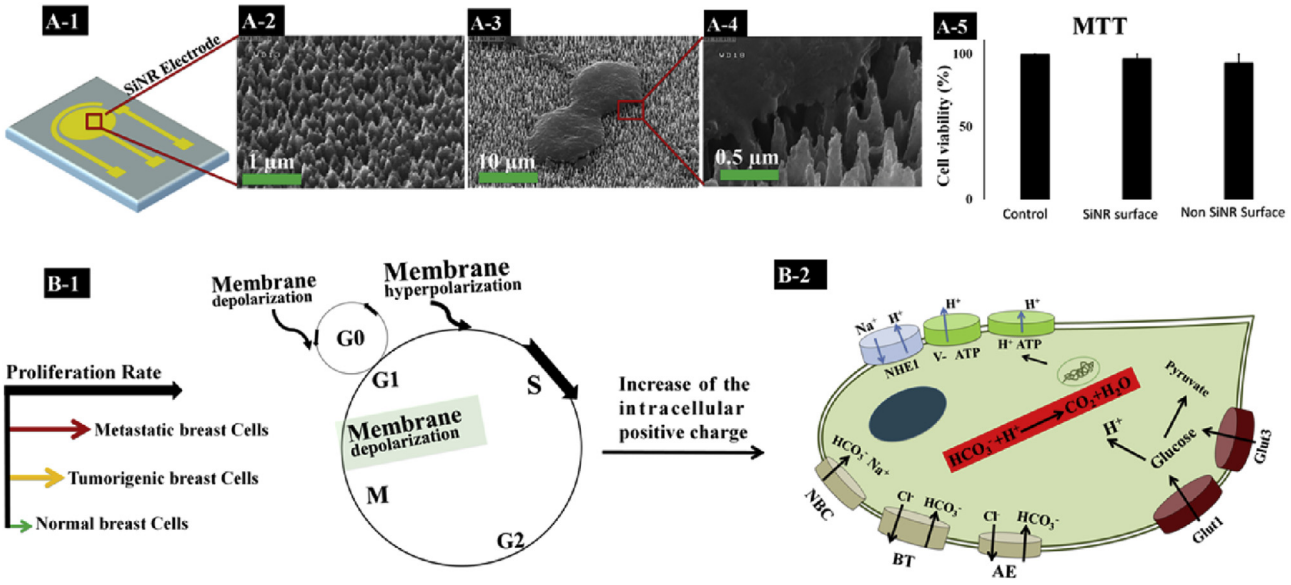

Fig. 4. Electron microscopy and graphical draw of the ion channels in the cells during acidification. (A-1) SEM image of the SiNR work electrode. (A-2) Image of a seeded cell on the work electrode in the mitotic sate. (A-3, 4) SEM images of Nano interface and increased interaction between cells and SiNR. (A-5) Biocompatibility of the work electrode analyzed with MTT assay. (B-1, 2) Graphical draw for the function of ion channels and the role of membrane depolarization and H+ ion exchange in the invasive cells during acidification.

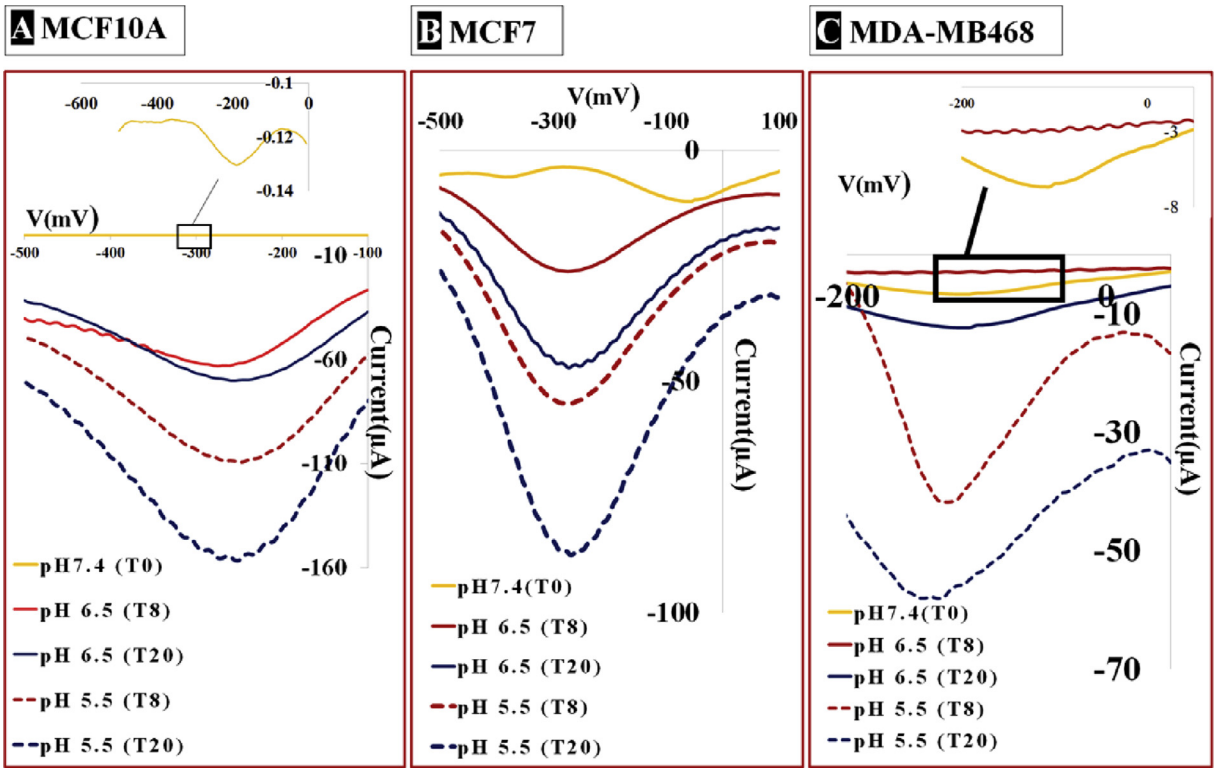

Fig. 5. DPV responses of (A) MCF10 (B) MCF7 and (C) MDA-MB468 cell lines incubated in different pH for various time intervals. The intensity of the peaks is quite sharper in normal cells and become lower in the progressive cancer cells.

neutralizer agent [24]. Small peak observed in CV profile of MCF7 cells at pH 6.5 indicating an elevation in the oxidation/reduction peak which implies that a small amount of released H^+ could be detected in the media of these cells due to the lower concentration of the entered $HCO3^-$ and their less invasive feature (Fig. 3 B2) [26].

To confirm our hypothesis that apoptosis was induced in this process, a complete set of biological assays including Annexin/PI (Fig. 7 A, B), cell cycle (Fig. 7 C, D), MMP (Fig. 8 A, B), NO_2 (Fig. 8 C1) and ROS (Fig. 8 C2) were carried out.

To further verify our results obtained by CV, we also performed differential pulse voltammetry (DPV) as an alternative approach for CV [27] by removing the common mode (baseline current) in the CV signal in order to observe the complete alterations of current (Fig. 5). Consistent with our previous data, these findings implied that acidosis state can be activated in normal breast (MCF10) cells in the acidic media leading to an enhanced electrochemical peak (Fig. 5 A); while the

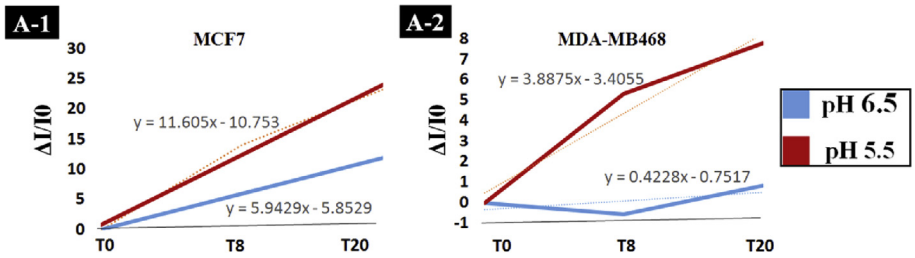

Fig. 6. Detection limit profiles of the SiNR electrochemical biosensor in sensing the acidic extracellular media are plotted in A1 and A2 panels, respectively. The detecting resolution followed the formulated regime is presented in each panel.

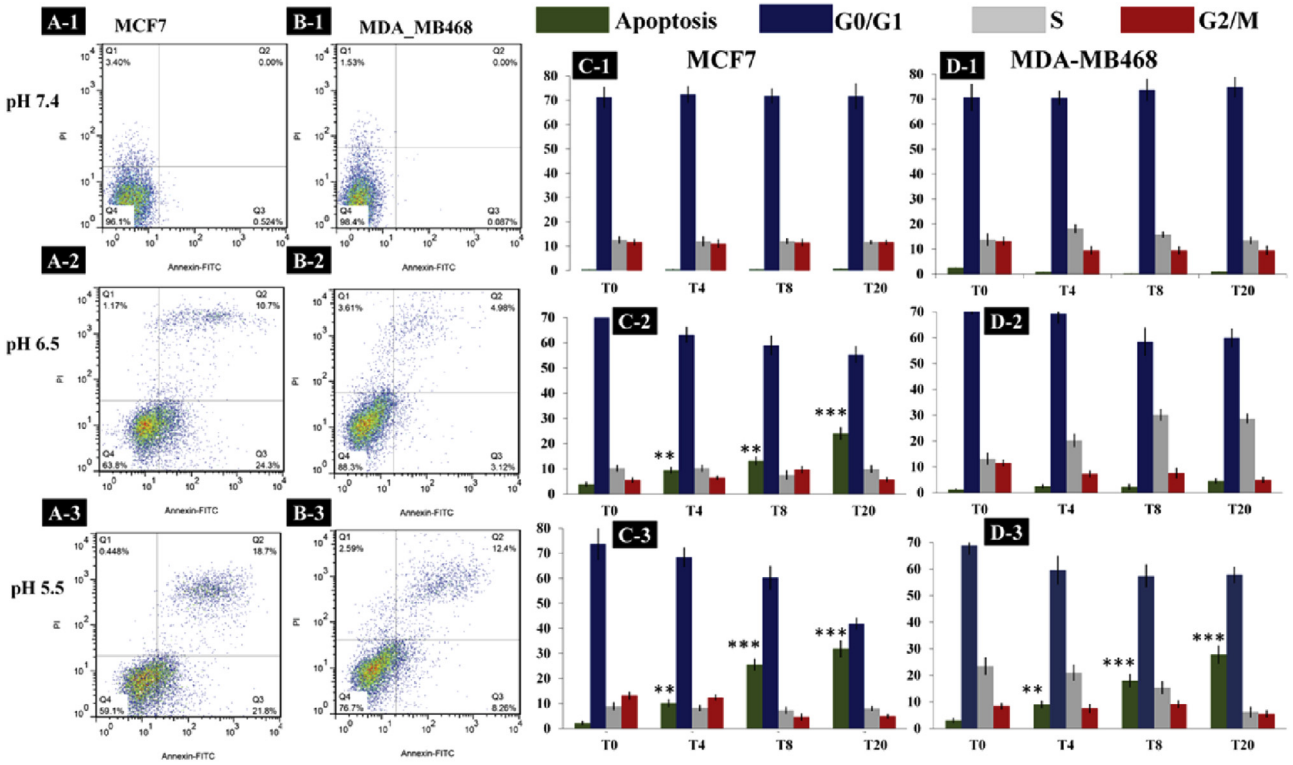

Fig. 7. Annexin-PI aasay shows the Apoptotic states of the cells in 4 states(Viable, early apoptose, late apoptose and necrosis). in pH 7.4 (A-1, B-1) the major of the cells was in the viable states as normally. MCF7 in the low acidic media(pH6.5) and High acidic media(pH5.5)cells entered to early and late apoptosis respectively (A-2,A-3). Invasice breast cancer cell (MDA-MB468) in the low acidic media in contrast of High acidic media (pH5.5) resisted to enter in apoptotic states and kept their viable features. (B-2, B-3). The results are expressed as mean ± SEM (N = 3), *p < 0.001 and p < 0.01 compared to the T0 group.

intensity of the peaks was diminished in breast cancer cells regarding their invasive stage (Fig. 5 B, C). Interestingly, DPV profile for MDA-MB468 cells showed a similar behavior in both normal and lower acidic ambient.

Fig. 6 presented the detection limit profiles of SiNR-based biosensor experimented for two types of assayed breast cancer cells. The pH dependent distinguished response of deice was recordable in 12th hr (T8) in which the slope of the sensitivity profile became changed in acidic pH for all type of the cells.

Fig. 6 revealed the differential changes in blocking current by cells (ΔI/I0) related to time. Due to different in ion-exchange features of cells, (ΔI/I0) is directly related to Δinterchangeable ion followed by sensor and based on Fig. 5 B,C in every time. The slope of equation in every sample revealed the ratio of current blocking and in the simple present ratio of cell's proliferation. MDA-MB 468 in the low acidic media (pH 6.5) has positive and low slope (0.4228) which is revealed the behavior of cells in this condition is similar to primary condition. Also we tested about 50000 cells in each assay but the dynamic range of the sensor could be increased to about 100000 cells in which the surface of the device got saturated. Hence, due to the mitotic rate of cancer cells, pre concentration of about 50000 and monitoring the responses for 48hr could resulted in non-saturated and desired achievements on effect of the pH.

3.3. Effect of acidic extracellular media on ANPI, cell cycling, mitochondrial membrane potential (MMP), NO_2^- production and intracellular ROS level

The ANPI results of MCF7 cells (Fig. 7 A1) revealed the meaningful reduction in the fraction of live cells after maintaining in pH6.5 and pH5.5. (Fig. 7 A2 vs. 7 A3). But the behavior of MDA-MB468 in the same acidic culturing media was differ in low pH media from MCF7 cells. ANPI result revealed that MDA-MB468 survived in lower pH.

The cell cycle analysis revealed that MCF7 in acidic media depending on pH the fraction of apoptosis has been increased and the cells could not maintain live function (Fig. 7 C). Also MDA-MB468 cells survived in low pH (6.5) and presented very minor decrease in the population of live cells (Fig. 7 D2).

We also measured the effect of acidic extracellular media on MMP as a main mitochondrial factor that controls the cellular processes. In

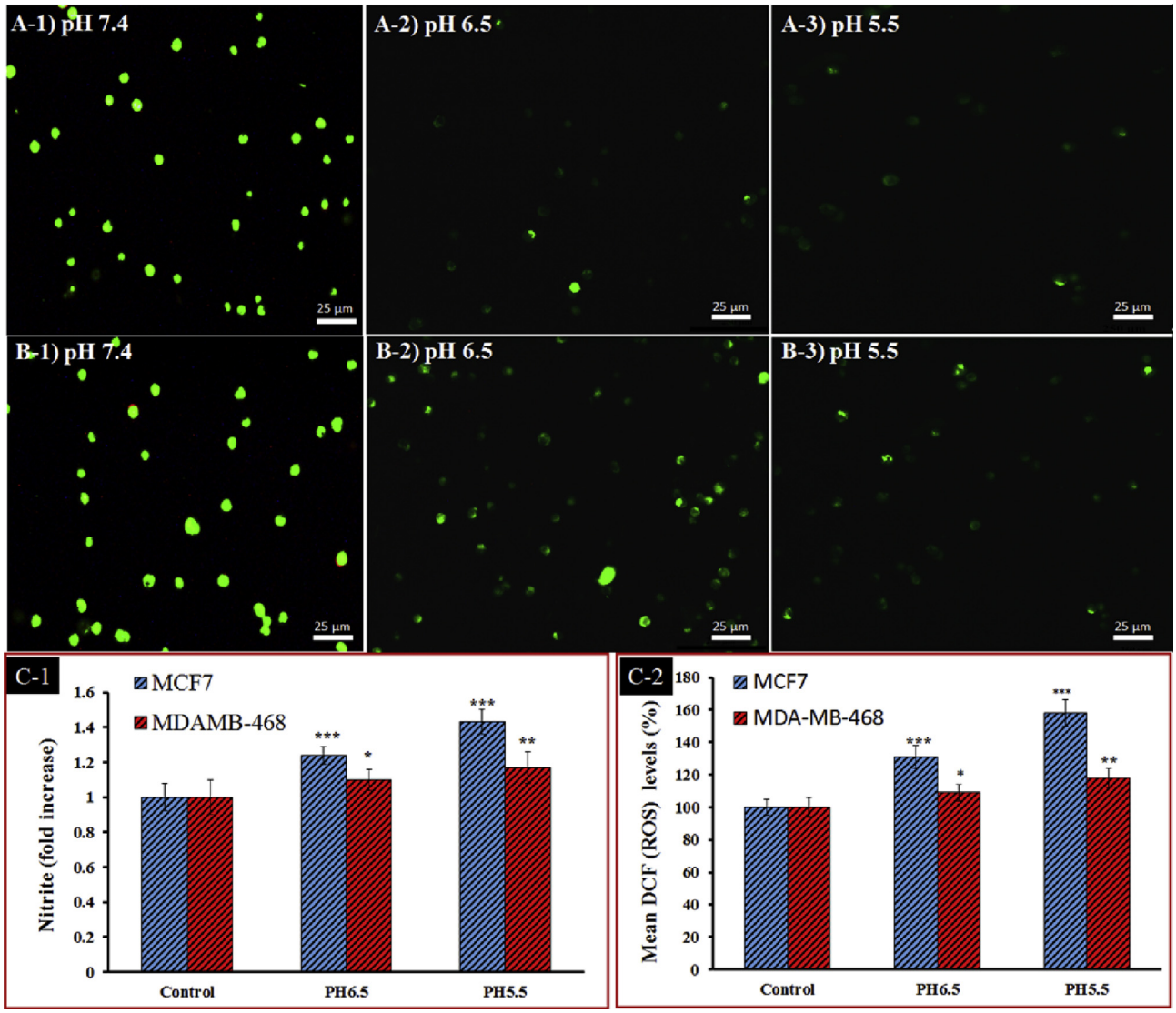

Fig. 8. The mitochondrial membrane potential (MMP) as well as release of NO and ROS showed in (A, B, C) that NO in low pH extracellular media increased but the ratio of this change in metastatic and non-metastatic cells connected to resistance of cells from apoptosis. MCF7 in pH6.5 and pH5.5 had more changes than MDA-MB468 in the same condition (C-1). Intracellular radicals ONO− and OH− had different pathway due to their metastatic properties (C-2).

fact, MMP reduction would lead to the initiation of apoptosis and the absence of Rhoda mine123 from the cells indicates the loss of MMP (Fig. 8 A, B). It is observable that incubating the cells in acidic media decreased the level of MMP in both MCF7 and MDA-MB468 but such reduction was more noticeable in MCF7 cells (Fig. 8 A2, A3 vs. 8 B2, B3).

Griess reagent was applied to study the effect of pH treatment on NO_2^- production in the breast cancer cell lines. Our observation revealed that over production of NO_2^- was more significant in MCF7 cells (1.3 ± 0.2, fold compared to the control). In confirmation with our previous results, at pH 6.5, no major NO_2^- over production was observed in MDA-MB468 cell line (Fig. 8 C1).

Similar to NO_2^- assay, ROS analysis demonstrated that the treatment of MCF7 cells in both acidic pH increased the intracellular ROS levels. Also, the increment in the level of ROS was milder in acidified MDA-MB468 cells (Fig. 8 C2).

4. Conclusion

Our results provide the evidence for the first time that the oxidation/reduction peaks recorded by electrochemical SiNR biosensor in the breast cells cultured in an acidified medium, are directly associated with the metastatic phenotypes of the cells. Normal cells, incubated in the acidic pH, revealed the extensive electrochemical peaks, whereas these peaks were reduced in the malignant breast cells. To underlie the related mechanism, we suggested that in the acidified media, breast cancer cells try to maintain their viability and acquire resistance to apoptosis, regarding their metastatic stage, by neutralizing the intracellular H^+ as a subsequent activation of BT and NBC transporters as well as $HCO3^-$ production. The method developed in this study would open a new avenue in the label-free detection of cancer cells based on the medium properties including pH.

References

[1] M. Turner, M. Londei, M. Feldmann, Human T cells from autoimmune and normal individuals can produce tumor necrosis factor, Eur. J. Immunol. 17 (1987) 1807–1814, https://doi.org/10.1002/eji.1830171220.
[2] R. Gupta, N.K. Chaudhury, Entrapment of biomolecules in sol-gel matrix for applications in biosensors: problems and future prospects, Biosens. Bioelectron. 22 (2007) 2387–2399, https://doi.org/10.1016/j.bios.2006.12.025.
[3] Radecka Hanna, Jerzy Radecki, Iwona Grabowska, Katarzyna Kurz?tkowska, Functional Nanoparticles for Bioanalysis, Nanomedicine, and Bioelectronic Devices, vol. 1, American Chemical Society, Washington, DC, 2012, , https://doi.org/10.

1021/bk-2012-1112.
[4] W.-W. Zhao, J.-J. Xu, H.-Y. Chen, Photoelectrochemical enzymatic biosensors, Biosens. Bioelectron. 92 (2017) 294–304, https://doi.org/10.1016/j.bios.2016.11.009.
[5] T. shu Chu, R. Lü, B. tong Liu, Reversibly monitoring oxidation and reduction events in living biological systems: recent development of redox-responsive reversible NIR biosensors and their applications in in vitro/in vivo fluorescence imaging, Biosens. Bioelectron. 86 (2016) 643–655, https://doi.org/10.1016/j.bios.2016.07.039.
[6] Y. Du, B. Li, H. Wei, Y. Wang, E. Wang, Multifunctional label-free electrochemical biosensor based on an integrated aptamer, Anal. Chem. 80 (2008) 5110–5117, https://doi.org/10.1021/ac800303c.
[7] M.S. Nikshoar, M.A. Khayamian, S. Ansaryan, H. Sanati, M. Gharooni, L. Farahmand, F. Rezakhanloo, K. Majidzadeh-A, P. Hoseinpour, S. Dadgari, L. Kiani-M, M. Saqafi, M. Gity, M. Abdolahad, Metas-Chip precisely identifies presence of micrometastasis in live biopsy samples by label free approach, Nat. Commun. 8 (2017) 2175, https://doi.org/10.1038/s41467-017-02184-x.
[8] M. Jacobs, S. Muthukumar, A. Panneer Selvam, J. Engel Craven, S. Prasad, Ultrasensitive electrical immunoassay biosensors using nanotextured zinc oxide thin films on printed circuit board platforms, Biosens. Bioelectron. 55 (2014) 7–13, https://doi.org/10.1016/j.bios.2013.11.022.
[9] P. Pancoska, B.I. Carr, Macro- and micro-environmental factors in clinical hepatocellular cancer, Semin. Oncol. 41 (2014) 185–194, https://doi.org/10.1053/j.seminoncol.2014.03.001.
[10] J. Xie, H. Wu, C. Dai, Q. Pan, Z. Ding, D. Hu, B. Ji, Y. Luo, X. Hu, Beyond Warburg effect – dual metabolic nature of cancer cells, Sci. Rep. 4 (2015) 4927, https://doi.org/10.1038/srep04927.
[11] Y. Kato, S. Ozawa, C. Miyamoto, Y. Maehata, A. Suzuki, T. Maeda, Y. Baba, Acidic extracellular microenvironment and cancer, Canc. Cell Int. 13 (2013) 89, https://doi.org/10.1186/1475-2867-13-89.
[12] M. Barathova, M. Takacova, T. Holotnakova, A. Gibadulinova, A. Ohradanova, M. Zatovicova, A. Hulikova, J. Kopacek, S. Parkkila, C.T. Supuran, S. Pastorekova, J. Pastorek, Alternative splicing variant of the hypoxia marker carbonic anhydrase IX expressed independently of hypoxia and tumour phenotype, Br. J. Canc. 98 (2008) 129–136, https://doi.org/10.1038/sj.bjc.6604111.
[13] A. Suzuki, T. Maeda, Y. Baba, K. Shimamura, Y. Kato, Acidic extracellular pH promotes epithelial mesenchymal transition in Lewis lung carcinoma model, Canc. Cell Int. 14 (2014) 129, https://doi.org/10.1186/s12935-014-0129-1.
[14] B. Alberts, A. Johnson, J. Lewis, M. Raff, K. Roberts, P. Walter, Ion Channels and the Electrical Properties of Membranes, (2002) https://www.ncbi.nlm.nih.gov/books/NBK26910/ , Accessed date: 15 October 2017.
[15] S. Zanganeh, S. Khosravi, N. Namdar, M.H. Amiri, M. Gharooni, M. Abdolahad, Electrochemical approach for monitoring the effect of anti tubulin drugs on breast cancer cells based on silicon nanograss electrodes, Anal. Chim. Acta 938 (2016) 72–81, https://doi.org/10.1016/j.aca.2016.07.042.
[16] J. Acker, A. Hensge, Chemical analysis of acidic silicon etch solutionsII. Determination of HNO3, HF, and H2SiF6 by ion chromatography, Talanta 72 (2007) 1540–1545, https://doi.org/10.1016/j.talanta.2007.02.005.
[17] H. Shashaani, M. Faramarzpour, M. Hassanpour, N. Namdar, A. Alikhani, M. Abdolahad, Silicon nanowire based biosensing platform for electrochemical sensing of Mebendazole drug activity on breast cancer cells, Biosens. Bioelectron. 85 (2016) 363–370, https://doi.org/10.1016/j.bios.2016.04.081.
[18] D.A.C. Saura, C. Sahu, Nanotoxicity: from in Vivo and in Vitro Models to Health Risks, John Wiley & Sons, 2009.
[19] B.R. You, W.H. Park, Gallic acid-induced lung cancer cell death is related to glutathione depletion as well as reactive oxygen species increase, Toxicol. Vitro 24 (2010) 1356–1362, https://doi.org/10.1016/j.tiv.2010.04.009.
[20] L. Wang, B. Wu, Y. Sun, T. Xu, X. Zhang, M. Zhou, W. Jiang, Translocation of protein kinase C isoforms is involved in propofol-induced endothelial nitric oxide synthase activation, Br. J. Anaesth. 104 (2010) 606–612, https://doi.org/10.1093/bja/aeq064.
[21] O. Kempski, F. Staub, M. Jansen, F. Schodel, A. Baethmann, Glial swelling during extracellular acidosis in vitro, Stroke 19 (1988) 385–392, https://doi.org/10.1161/01.STR.19.3.385.
[22] S. Berzingi, M. Newman, H.-G. Yu, Altering bioelectricity on inhibition of human breast cancer cells, Canc. Cell Int. 16 (2016) 72, https://doi.org/10.1186/s12935-016-0348-8.
[23] A.A. Marino, I.G. Iliev, M.A. Schwalke, E. Gonzalez, K.C. Marler, C.A. Flanagan, Association between cell membrane potential and breast cancer, Tumor Biol. 15 (1994) 82–89, https://doi.org/10.1159/000217878.
[24] M. Yang, W.J. Brackenbury, Membrane potential and cancer progression, Front. Physiol. 4 (2013) 185, https://doi.org/10.3389/fphys.2013.00185.
[25] M. Damaghi, J.W. Wojtkowiak, R.J. Gillies, pH sensing and regulation in cancer, Front. Physiol. 4 (2013) 370, https://doi.org/10.3389/fphys.2013.00370.
[26] I.D.G. Rongbao Zhao, Ndeye Diop-bove, Michele Visentin, NIH Public Access, (2014), https://doi.org/10.1146/annurev-nutr-072610-145133.Mechanisms.
[27] N. Aravindan, S. M.V, Differential pulse voltammetry as an alternate technique for over oxidation of polymers: application of electrochemically synthesized over oxidized poly (Alizarin Red S) modified disposable pencil graphite electrodes for simultaneous detection of hydroqui, J. Electroanal. Chem. 789 (2017) 148–159, https://doi.org/10.1016/j.jelechem.2017.02.037.